N-ary Mathematical Morphology

Emmanuel Chevallier[a], Augustin Chevallier[b], Jesús Angulo[a]

[a] MINES ParisTech, PSL-Research University,
CMM-Centre de Morphologie Mathématique, France
[b] Ecole Normale Supérieur de Cachan, France
emmanuel.chevallier@mines-paristech.fr

Abstract. Mathematical morphology on binary images can be fully described by set theory. However, it is not sufficient to formulate mathematical morphology for grey scale images. This type of images requires the introduction of the notion of partial order of grey levels, together with the definition of sup and inf operators. More generally, mathematical morphology is now described within the context of the lattice theory. For a few decades, attempts are made to use mathematical morphology on multivariate images, such as color images, mainly based on the notion of vector order. However, none of these attempts has given fully satisfying results. Instead of aiming directly at the multivariate case we propose an extension of mathematical morphology to an intermediary situation: images composed of a finite number of independent unordered categories.

1 Introduction

A key idea of mathematical morphology is the extension and the reduction of the surface of the different objects of an image over their neighbors. This idea leads naturally to the two basic morphological operators in binary images.

Binary images. In such images, there are only two kinds of objects: black or white objects. Two dual and adjoint operators have been defined: the erosion and the dilation. The erosion extends the black objects over the white objects, the dilation extend the white objects over the black objects. Formally, a binary image can be seen as a support set Ω, and X a subset of Ω. Let B be a subset of Ω called the structuring element. We assume that Ω disposes of a translation operation. The erosion $\varepsilon_B(X)$ and the dilation $\delta_B(X)$ of X according to a structuring element are defined as follows [4,6]:

$$\varepsilon_B(X) = \bigcap_{y\in B} X_{-y} = \{p \in \Omega \,:\, B_p \subset X\} = \left\{x \,:\, \forall p \in \check{B}, x \in X_p\right\}, \quad (1)$$

$$\delta_B(X) = \bigcup_{y\in B} X_y = \{x+y \,:\, x \in X, y \in B\} = \left\{p \in \Omega \,:\, X \cap \check{B}_p \neq \emptyset\right\}. \quad (2)$$

where $\check{X} = \{-x \,:\, x \in X\}$ is the transpose of X (or symmetrical set with respect to the origin O) and $X_p = \{x+p \,:\, x \in X\}$ the translate of X by p. For the

sake of simplicity, we limit the rest of our notation to symmetric structuring elements: $B = \check{B}$.

Grey-scale images. With the apparition of grey-scale images, mathematical morphology was reformulated in terms of inf and sup convolution where the kernel is the structuring element B [6]. An image is now considered as a function I defined as

$$I : \begin{cases} \Omega \to V \\ p \mapsto I(p) \end{cases}$$

where V is the set of grey-levels, which can be generally assumed as a subset of the real line $V \subset \mathbb{R}$. Grey-scale flat erosion and dilation of I by structuring element B are now defined as follows:

$$\varepsilon_B(I)(p) = \inf_{q \in B_p} \{f(q)\}, \quad \delta_B(I)(p) = \sup_{q \in B_p} \{f(q)\}.$$

In this framework, each grey-level is not fully considered as an independent color (i.e., a different category) but simply as an intermediary level between black and white. This point of view is actually justified when interesting objects of the images are local extrema.

Fig. 1. Grey-level morphological processing: (a) original image I, (b) closing $\varphi_B(I)$, (c) opening $\gamma_B(I)$.

Let us see what happens in the situation depicted in Fig. 1. It corresponds to process a rather simple grey-level by a closing and an opening. We recall that the closing of I by B is the composition of a dilation followed by a erosion; i.e., $\varphi_B(I) = \varepsilon_B(\delta_B(I))$. The opening is just the dual operator; i.e., $\gamma_B(I) = \delta_B(\varepsilon_B(I))$. Closing (resp. opening) is appropriate to remove dark (resp. bright) structures smaller than the structuring element B. This behavior is based on the fact that the dilation "reduces" dark structures by B while the erosion "restores" the dark structures which are still present.

In the current example, it is not possible to remove the central grey spot using erosion and dilation with B larger than the spot size. This grey spot is not considered as an interesting object in itself but simply as an intermediary value between the black object and the white object. If this assumption is often coherent, this is not always the case.

Let consider the grey-scale image in Fig. 2(a). In this image, each grey level has the same semantic level: each represents a different component, sometimes called a phase. However, in the morphological grey-scale framework, the grey is processed as an intermediary level. It is possible to replace each grey level by a

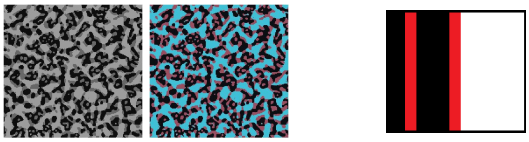

(a) (b) (c)

Fig. 2. (a) A three independent grey-scale image and (b) the same image where the grey values has been replaced by colors. (c) Example of multivariate (color) image.

color, see Fig. 2(b). We would like then to process both images using the same approach.

Multivariate images. For multivariate images, no canonical framework has yet appeared. Most processing consist in endowing the structure with a partial order relationship. The structure has to be a complete lattice in order to define erosion and dilation in terms of inf and sup. The notion of order induces the notion of intermediary level as in the precedent framework. However, the notion of intermediary levels often leads to non-intuitive situations, see example in Fig. 2(c). As the red usually has a real signification in terms of a particular class of objects, it is very natural to try to remove the red spot, which is not possible using generic classical morphology. The more the image has a complex semantic structure, such as a color image, the more it is difficult to find a lattice structure which makes every interesting object an extremum.

Aim and paper organization. Historically, mathematical morphology has been generalized from binary to grey scale, and then to multi-variate images. However, the gap between grey-scale and color is much more significant than the gap between binary and grey-scale. As we discussed previously, the grey-scale structure only enables to define intermediary colors between two references. This structure is obviously too weak to describe color information. Note that to simplify the vocabulary, we use the notion of color for any non-scalar valuation of the pixels on the image.

Before extending mathematical morphology to color images, we might want to define a coherent approach for mathematical morphology with n independent unordered colors, without considering them as intermediary levels. This is the aim of this paper. Then only, we might try in the future to define mathematical morphology for the full color space. The difference between the frameworks can be interpreted in term of a change of metric on the value space:

- grey-scale framework: $\forall(i,j),\ \ d(color_i, color_j) = |i-j|$;
- $n-$ary framework: $\forall(i,j),\ \ d(color_i, color_j) = 1$.

Our paper is not the first to consider the problems of classical mathematical morphology for images composed of independents categories. Authors of [1] have very similar motivations but the development we propose is different. In contrast to operators proposed in [1] or labelled openings from [2], we are interested in filling gaps left by anti-extensive operators. We note that the theory of

morphological operators for partitions [8] and hierarchies of partitions [5] is not compatible with our framework.

The rest of the paper is organized as follows. A proposition of n-ary morphological operators and a study of their theoretical properties in Sections 2 and 3. Some applications to image filtering are discussed in Section 4. Section 5 of conclusions closes the paper.

2 n-ary morphological operators

Let us come back to the key idea of mathematical morphology is to reduce and extend objects over their neighbors. In the case of binary images, two operations where introduced: the erosion extends the black over the white and the dilation extends the white over the black. In a general way, we would like to allow to reduce and extend the surface of each category of object. This makes four theoretic operations in the binary case, reduced to two in practice due to the coincidence of certain operations: reducing the black is the same as extending the white and conversely. This duality is one of the basic principle of binary morphology.

2.1 Dilation and erosion of color i

Let I be an n-ary image defined as

$$I : \begin{cases} \Omega \to \{1, 2, \cdots, n\} \\ p \mapsto I(p) \end{cases}$$

In the $n-$ary case, it seems natural to try to introduce the corresponding pair $(\varepsilon_i, \delta_i)$ of operators for each color i. Erosion ε_i is the operator that reduces the surface of the objets of color i, and dilation δ_i the operator that extends the color i. Above $n > 2$, we unfortunately lose the duality between operations, such that the number of elementary operators is then equal to $2n$. Let us formulate more precisely these operators.

The *dilation of color i on image I by structuring element B* presents no difficulty:

$$\delta_i(I; B)(x) = \begin{cases} I(x) & \text{if } \forall p \in B_x, I(p) \neq i \\ i & \text{if } \exists p \in B_x, I(p) = i \end{cases} \tag{3}$$

$\delta_i(I; B)$ extends objects of color i over their neighbors. The case of the erosion presents more theoretical difficulties. Indeed, if we want to reduce the objects of color i, we need to decide how to fill the gaps after the reduction.

Let us first define the erosion for pixels where there are no ambiguities. Thus the *erosion of color i on image I by structuring element B* is given by

$$\varepsilon_i(I; B)(x) = \begin{cases} I(x) & \text{if } I(x) \neq i \\ i & \text{if } \forall p \in B_x, I(p) = i \\ \theta(x, I) & \text{otherwise} \end{cases} \tag{4}$$

We will address later definition of $\theta(x, I)$. Sections 2.2 and 2.3 are independent of θ. Although the image is a partition of Ω the proposed framework differs from [8].

2.2 Opening and closing of color i

Once the dilation and erosion have been defined, we can introduce by composition of these two operators the *opening and the closing on I by B of color i* respectively as

$$\gamma_i(I;B) = \delta_i \circ \varepsilon_i = \delta_i\left(\varepsilon_i(I;B);B\right), \tag{5}$$
$$\varphi_i(I;B) = \varepsilon_i \circ \delta_i = \varepsilon_i\left(\delta_i(I;B);B\right). \tag{6}$$

Let us set a few notations used in the following. If ϕ is an operator, let ϕ^k be $\phi \circ .... \circ \phi$ the iteration of ϕ, k times. Let $\phi_{|A}$ be the restriction of ϕ to the subset A. Let us set $E_i^I = I^{-1}(i)$. To simplify, $\mathbf{1}_{E_i^I}$ will be noted $\mathbf{1}_i^I$.

We have the following property of stability.

Proposition 1. *Opening and closing of color i are idempotent operators, i.e.,*

$$\gamma_i(I;B) = \gamma_i^2(I;B),$$
$$\varphi_i(I;B) = \varphi_i^2(I;B).$$

Proof. Since the binary opening is idempotent, one has $E_i^{\gamma_i(I)} = E_i^{\gamma_i^2(I)}$. Furthermore we have that $E_j^{\gamma_i(I)} \subset E_j^{\gamma_i^2(I)}$, for all $j \neq i$. Since sets $(E_i)_i$ from a partition of the support space, necessarily $E_j^{\gamma_i(I)} = E_j^{\gamma_i^2(I)}$, $\forall j$. Indeed, if all the elements of a partition are extensive, then they all remain stable. Then $\gamma_i = \gamma_i^2$.

Properties cannot directly be transported by duality, as in binary morphology, however the property remains true for the closing. We first show the binary property $\varepsilon\delta\varepsilon = \varepsilon$. The binary erosion and opening can be written as

$$\varepsilon_B(X) = \cup_{B_x \subset X}\{x\}, \quad \text{and} \quad \gamma_B(X) = \cup_{B_x \subset X} B_x.$$

Then $\varepsilon(\gamma(X)) = \cup_{B_x \subset \gamma(X)}\{x\}$. Since $\{B_x \subset \gamma(X)\} = \{B_x \subset \cup_{B_x \subset X} B_x\} = \{B_x \subset X\}$, then $\varepsilon(\gamma(X)) = \varepsilon(X)$. Thus, $\varepsilon\delta\varepsilon = \varepsilon$ and by duality, $\delta\varepsilon\delta = \delta$. Then $E_i^{\delta_i} = E_i^{\delta_i\varepsilon_i\delta_i}$. It can be shown that $E_j^{\delta_i} \subset E_j^{\delta_i\varepsilon_i\delta_i}$ for all $j \neq i$. Using the same reasoning as in the proof for the opening, we have that for all j, $E_j^{\delta_i} = E_j^{\delta_i\varepsilon_i\delta_i}$. In other words, $\delta_i\varepsilon_i\delta_i = \delta_i$. Thus $\varepsilon_i\delta_i\varepsilon_i\delta_i = \varepsilon_i\delta_i$, or equivalently $\varphi_i = \varphi_i^2$.

Fig. 3. Opening and closing on a 3-ary image: (a) original image I, (b) opening of red color $\gamma_{red}(I;B)$, (c) closing of black color $\varphi_{black}(I;B)$.

2.3 Composed n-ary filters

We can now try to define color filters from the openings and the closings of color i. In binary morphology, the simplest filters are of the following form: $\gamma \circ \phi$ and $\phi \circ \gamma$. In the n-ary framework, with $n = 2$, they can be rewritten as

$$\gamma_1 \circ \gamma_2 = \phi_2 \circ \phi_1, \quad \text{and} \quad \gamma_2 \circ \gamma_1 = \phi_1 \circ \phi_2.$$

The opening removes peaks smaller than the structuring element and the closing removes holes, which are dual notions in binary morphology. However, peaks and holes are no longer a dual notion in n-ary morphology with $n > 2$. Fig. 3 illustrates the difference between openings and closings on a 3-ary image: three colors, black, white and red. The structuring element is a square whose size is half of the width of the red line. Removing the red line using φ_{black} requires a structuring element twice bigger than with γ_{red}.

As a good candidate to filter out small object of a color image I, independently of the color of the objects, we introduce the operator ψ, named *composed n-ary filter by structuring element B*, defined as

$$\psi(I;B) = \gamma_n(I;B) \circ \gamma_{n-1}(I;B) \circ \cdots \circ \gamma_1(I;B). \tag{7}$$

Unfortunately on the contrary to $\gamma \circ \phi$ in binary morphology, ψ is generally not idempotent. Worst, the sequence ψ^k do not necessarily converge. However we still have a stability property for relevant objects. Let us be more precise.

Proposition 2. *Let Ω be a finite set. Given a structuring element B, the interior with respect to B of the composed n-ary filter $\psi(I;B)$ converges for any image I, i.e.,*

$$\forall i, \varepsilon(E_i^{\psi^k}) \text{ converges .}$$

Proof. Since $\varepsilon = \varepsilon \circ \delta\varepsilon$, $\forall i$, $\varepsilon(E_i^{\psi^k}) = \varepsilon(E_i^{\gamma_i \circ \psi^k})$. Furthermore, since $\varepsilon(E_i^{\psi^k}) \subset \varepsilon(E_i^{\gamma_j \circ \psi^k})$, we have that $\forall i, \varepsilon(E_i^{\psi^k}) \subset \varepsilon(E_i^{\psi^{k+1}})$. Since Ω is a finite set, $\varepsilon(E_i^{\psi^k})$ converges.

This property ensures that the variations between ψ^k and ψ^{k+1} do not affect the interior of objects and is only limited to boundaries. Nevertheless, as we shown in section 4, ψ^k is almost always stable after a few iterations.

2.4 n-ary geodesic reconstruction

The binary reconstruction can be transposed in the n-ary framework as follows. Given two color images R and M, for each color i,

- Perform a binarisation of the reference R and the marker M between i and $\complement i$, which correspond respectively to binary images X_i and Y_i.
- Compute $\gamma^{\text{rec}}(X_i; Y_i)$, that is the binary geodesic reconstruction of the marker in the reference.

Then, the *n-ary geodesic reconstruction of color reference R by color marker M* is given by

$$\gamma^{\text{rec}}(R;M)(x) = \begin{cases} i & \text{if } x \in \gamma^{\text{rec}}(X_i;Y_i) \\ M(x) & \text{if } \forall i,\ x \notin \gamma^{\text{rec}}(X_i;Y_i) \end{cases}$$

Fig.4 illustrates the difference between classical geodesic reconstruction and the proposed n-ary reconstruction. For the classical reconstruction, the 3 colors image is simply viewed as a grey-scale image.

(a) (b) (c) (d)

Fig. 4. Geodesic reconstruction of a 3-ary image: (a) reference image R, (b) marker image M, (c) classical grey-scale reconstruction, (d) n-ary reconstruction $\gamma^{\text{rec}}(R;M)$.

The aim of this definition is to symmetrize colors. In Fig.4 (d), the grey object is considered as an object in itself. The proposed reconstruction is a connected operator in the sense of [9]

3 On the choice of an erosion of color i

Before any application, we need to come back to the erosion problem. More precisely, we need to define a consistent rule to fill the space created by the erosion operation.

First of all, we note that the definition in Eq. (8) of the erosion of color i ε_i does not indicate how to behave on the following set:

$$A = \{x \mid I(x) = i \text{ and } \exists p \in B_x \text{ such that } I(p) \neq i\}.$$

For points $x \in A$ we have to decide by which color to replace color i and therefore to define ε_i on A, i.e.,

$$\varepsilon_i(I;B)(x) = \begin{cases} I(x) & \text{if } I(x) \neq i \\ i & \text{if } \forall p \in B_x, I(p) = i \\ ? & \text{if } x \in A \end{cases} \tag{8}$$

Many alternatives are possible. Two criteria have to be taken into account: (i) the direct coherence in terms of image processing, and (ii) the number of morphological properties verified by the erosion, such as $\varepsilon_i(I;kB) = \varepsilon_i^k(I;B)$ where $kB = \{kx \mid x \in B\}$ (i.e., homothetic of size k). Let us consider in particular the three following rules for $x \in A$:

1. **Fixed-color erosion:** Erosion always fills the gaps with color 1 (or any other fixed color):

$$\varepsilon_i(I;B)(x) = 1. \tag{9}$$

2. **Majority-based erosion:** Erosion takes the value of the major color different from i in the structuring element B:

$$\varepsilon_i(I;B)(x) = min(\arg\max_{j\neq i}(\text{Card}\,\{p \in B_x | I(p) = j\})). \tag{10}$$

3. **Distance-based erosion:** Erosion replaces color i by the closest color on the support space Ω:

$$\varepsilon_i(I;B)(x) = min(\arg\min_{j\neq i} d_x^j). \tag{11}$$

where $d_x^j = \inf\{\|x-p\|_\Omega \mid p \in \Omega,\ I(p) = j\}$

The majority-based erosion (10) and distance-based erosion (11) are initially not defined in case of equality. Hence the apparition of the *min*. Obviously, fixed-color erosion (9) satisfies $\varepsilon_i(I;kB) = \varepsilon_i^k(I;B)$, but is not coherent in terms of image processing.

Fig. 5. Comparison of erosions of black color: (a) original image I, (b) erosion $\varepsilon_{black}(I;B)$ using majority-based formulation (10), (c) erosion $\varepsilon_{black}(I;B)$ using distance-based formulation (11). Let l be the width of the red line, the structuring element B is a square whose size is now between l and $2l$. (d) iterated black erosion $\varepsilon_{black}^2(I;B)$ using majority-based formulation, (e) erosion $\varepsilon_{black}(I;2B)$ using majority-based formulation.

Majority-based erosion and distance-based erosion both look potentially interesting in terms of image processing; however, as shown in the basic example of Fig. 5, majority-based erosion (to compare Fig. 5(b) to Fig. 5(c)) can produce unexpected results. The same example, now Fig. 5(d) and Fig. 5(e), shows that majority-based erosion do not satisfies $\varepsilon_i(I;kB) = \varepsilon_i^k(I;B)$.

Let us formalize the iterative behavior of the distance-based erosion by the following result on isotropic structuring elements.

Proposition 3. *Let (Ω, d) be a compact geodesic space and I a n-ary image on Ω. For any $R_1, R_2 > 0$ the distance-based erosion of color i satisfies:*

$$\varepsilon_i(I;B_{R_1+R_2}) = \varepsilon_i(I;B_{R_2}) \circ \varepsilon_i(I;B_{R_1}).$$

where B_R is the open ball of radius R.

Proof. For the sake of notation, let $X = E_i^I$ and $X_j = E_j^I$, for $j \neq i$. Let $X' = \{x \in X | d(x, \complement X) \geq R_1\}$, X' is the binary eroded of X. Let $proj_X(a) =$

$\{b|b \in \overline{\complement X}, d(a,b) = d(a,\complement X)\}$ with $\overline{A}$ the closure of A. Let $\mathcal{P} = \{X_j\}$ and for $a \in \Omega$, $I_a^{\mathcal{P}} = \{j|\exists b \in proj_X(a) \cap \overline{X_j}\}$. Let $X'_j = \{a \notin X'|proj_X(a) \cap \overline{X_j} \neq \emptyset\}$ and $\mathcal{P}' = \{X'_j\}$. Using the property of the *min* function, $min(A \cup B) = min(\{min(A), min(B)\})$, it can be shown that $I_a^{\mathcal{P}} = I_a^{\mathcal{P}'}$ for all $a \in X'$ implies proposition 3.

- Let $j \in I_a^{\mathcal{P}}$. Thus, $\exists b \in proj_X(a) \cap \overline{X_j}$. Let γ be a geodesic joining a and b with $\gamma(0) = b$ and $\gamma(d(a,b)) = a$. Let $c = \gamma(R_1)$. For all $x \in \gamma([0, R_1[)$, $x \notin X'$ and $b \in proj_X(x)$. Hence $x \in X'_j$ and $c \in \overline{X'_j}$. The triangle inequality gives $c \in proj_{X'}(a)$. Indeed, assuming that $c \notin proj_{X'}(a)$ easily leads to $b \notin b \in proj_X(x)$. Thus, $j \in I_a^{\mathcal{P}'}$.
- Let $j \in I_a^{\mathcal{P}'}$. Thus, $\exists c \in proj_{X'}(a) \cap \overline{X'_j}$. By definition of the closure, $\exists c_n \to c, c_n \in X'_j$. $c_n \in X'_j \Rightarrow (\exists d_n \in proj_X(c_n), d_n \in \overline{X_j})$. The compact assumption enables us to consider that $d_n \to d$ (it is at least valid for a sub-sequence). $d \in \overline{X_j}$. By continuity, $d(d,c) = lim(d_n, c_n) = lim(\complement X, c_n) = d(\complement X, c)$. Thus, $d \in proj_X(c)$. Proposition 4 tells us that $d \in proj_X(a)$. Hence $j \in I_a^{\mathcal{P}}$.

Thus, $I_a^{\mathcal{P}} = I_a^{\mathcal{P}'}$.

Proposition 4. *Using the notation introduced in the demonstration of proposition 3:*

$$\forall a \in X', \forall c \in proj_{X'}(a), \forall d \in proj_X(c), d \in proj_X(a).$$

Proof. Let $a \in X', c \in proj_{X'}(a), d \in proj_X(c)$.

- Since X' is closed, $\complement X'$ is open and the existence of geodesics implies that $c \notin \complement X'$. Hence $c \in X'$ and $d(c, \complement X) \geq R_1$. Since c is a projection on $\complement X'$, we have $c \in \overline{\complement X'}$, $d(c, \complement X) \leq R_1$. Hence $d(c, \complement X) = R_1$ and $d(c,d) = R_1$.
- Let $b \in proj_X(a)$ and γ a geodesic such that $\gamma(0) = a$ and $\gamma(d(a,b)) = b$. Let $c' = \gamma(sup\{t|\gamma(t) \in X'\})$. Since X' is closed, $c' \in X'$. We have $d(c', \complement X) \geq R_1$. Since $c' \in \overline{\complement X'}$, $d(a,c') \geq d(a, \complement X') = d(a,c)$. Thus, $d(a,b) = d(a,c') + d(c',b) \geq d(a,c) + d(c', \overline{\complement X}) = d(a,c) + d(c', \complement X) \geq d(a,c) + R_1 = d(a,c) + d(c,d) \geq d(a,d)$. Hence $d \in proj_X(a)$.

Note that in a compact subset of a vector space, since proposition 3 is valid for any norm, the property holds for any convex structuring element. Note also that 3 is based on a metric definition of the erosion. For vector spaces norms, this erosion is identical to the translation based erosion. According to this discussion, in all what follows we adopt distance-based erosion.

4 Applications to image filtering

In the first case study, depicted in Fig. 6 and Fig. 7, we consider the behavior and interest of the composed n-ary filter $\psi(I;B)$. The aim is to filter out objects smaller than the structuring element B of the 4-ary (color) image Fig. 6(a). Results in Fig. 6(b) and (c) are respectively the classical color operator $\gamma_B \circ \varphi_B$ and

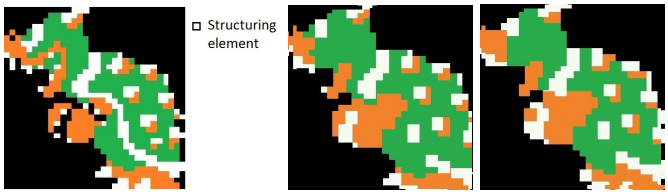

Fig. 6. Morphological filtering of a 4-ary image: (a) original color image I and structuring element B, (b) color operator $\gamma_B \circ \varphi_B$ using a color order (c) color operator $\varphi_B \circ \gamma_B$ using same order.

$\varphi_B \circ \gamma_B$ based on an arbitrary order. Alternative composed n-ary filter $\psi(I;B)$, which correspond to different permutations of the composition of openings of color i. On the one hand, note that in all the cases, the iterated filter converges rather fast to a stable (idempotent) result ant that the difference between the first iteration and the final result are rather similar. On the other hand, the different permutations produce different results, however in all the cases, the small objects seems better removed than in the case of the classical color order operators.

The second example, given in Fig. 8 attempts to regularize the 3-ary image, by removing small objects without deforming the contours of the remaining objects. More precisely, Fig. 8(a) represents the electron microscopy image of a ceramic eutectic, with three different phases after segmentation. The filtering process is composed of two steps: morphological size filter followed by geodesic reconstruction. We compare the result of filtering the color image according to two pipelines: (i) color total order framework, Fig. 8(b), where the filter is an opening by reconstruction composed with a closing by reconstruction; (ii) n-ary framework, Fig. 8(d), where the marker is a n-ary filter $\psi(I;B)$ followed by a n-ary geodesic reconstruction. In the case of the color ordering, black and blue are extreme color whereas red is the intermediary color. As we can observe, using the order-based approach all red objects that lay between black and blue objects are not extracted. Both n-ary and color total order frameworks give the same results for the blue grains. This corresponds to the fact that, in the color order, blue is an extreme color whereas red is an intermediary. Therefore the n-ary framework provides a more symmetric processing of all the colors.

The last example is a classification image from the brain. Fig. 9 (a) is a result of a classification where the red represents the grey matter, the green represents the white matter and the blue represents the cerebrospinal fluid. The processing is same as for the second example. The miss-classified white matter around the brain and some miss-classified grey matter spots around the cerebrospinal fluid are successfully removed by the n-ary framework, whereas they remain after the classical processing.

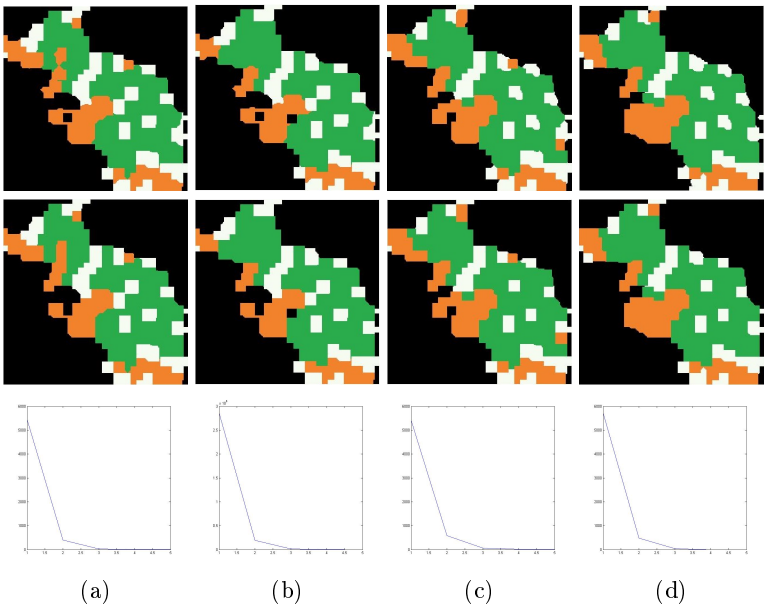

Fig. 7. n-ary processing of Fig. 6 (a). first row: composed n-ary filter $\psi(I;B)$, second row: iterated composed n-ary filter $\psi^k(I;B)$ until convergence, third row: convergence speed w.r.t. to k. Column (a) $\psi(I;B) = \gamma_1 \circ \gamma_2 \circ \gamma_3 \circ \gamma_4$, (b) $\psi(I;B) = \gamma_2 \circ \gamma_1 \circ \gamma_3 \circ \gamma_4$, (c) $\psi(I;B) = \gamma_3 \circ \gamma_4 \circ \gamma_1 \circ \gamma_2$, (d) $\psi(I;B) = \gamma_4 \circ \gamma_3 \circ \gamma_2 \circ \gamma_1$.

5 Conclusions and perspectives

We proposed here an approach to extend mathematical morphology to images composed of n independent levels. The approach presents two key particularities: first, the increase of the number of elementary operators, second, the absence of a notion of background or an indeterminate class. The absence of background or indeterminate class transforms the problem into a problem of gap filling. We prove that some of the elementary properties of standard morphological operators are preserved, such as the idempotence of openings and closings per color. Despite its quasi experimental validity, the main lost property is the granulometric semigroup. Beyond the mathematical properties, one of the natural consequences of this n-ary framework is the definition of a new reconstruction operator. The main application of the proposed operators is the filtering of small objects, the presented examples demonstrate the relevance of the n-ary operators. Our immediate research will focus on the recovery of the "granulometry property". In a second step, we plan to extend our applications to other classification images such as classified satellite images. Then in a third step, we will investigate the extension of the defined operators to the case of a fuzzy mixture between independent unordered categories.

Acknowledgement. We would like to thank Jasper van de Gronde, for the multiple discussions and constructive suggestions during our academic visits.

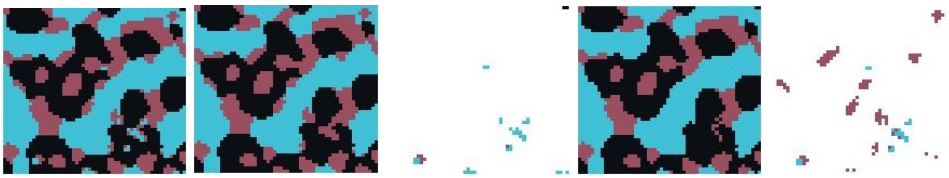

Fig. 8. Image size-regularization: (a) original image I, (b) classical order-based filtering, (c) residue between (a) and (b), (d) n-ary based filtering, (e) residue between (a) and (d). See the text for details.

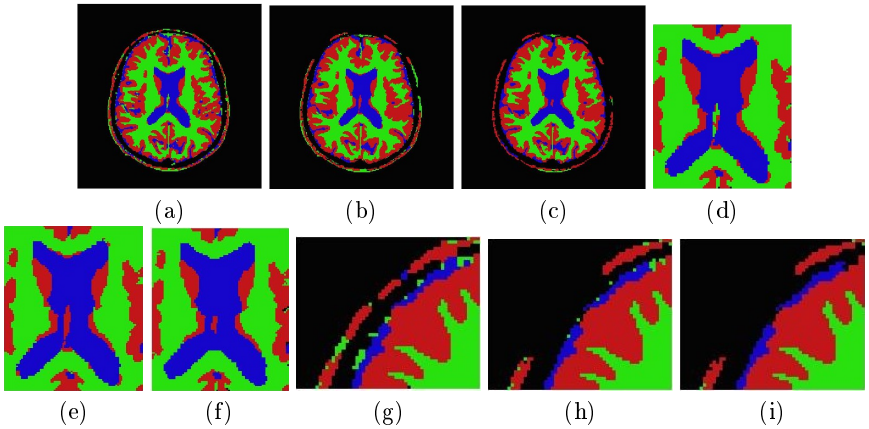

Fig. 9. Image size-regularization: (a) original image I, (b) classical order-based filtering, (c) n-ary based filtering, (d) zoom-in (a), (e) zoom-in (b), (f) zoom-in (c), (g) zoom-in (a), (h) zoom-in (b),(i) zoom-in (c). See the text for details.

References

1. C. Busch, M. Eberle. *Morphological Operations for Color-Coded Images.* Proc. of the EUROGRAPHICS'95, Computer Graphics Forum, Vol. 14, No. 3, C193–C204, 1995.
2. A. Hanbury, J. Serra. Morphological operators on the unit circle. IEEE Trans. Image Processing, 10(12):1842–50, 2001.
3. H.J.A.M. Heijmans. *Morphological image operators.* Academic Press, Boston, 1994.
4. G. Matheron. *Random Sets and Integral Geometry.* Wiley, New York, 1975.
5. F. Meyer. Adjunctions on the lattice of hierarchies. *HAL,* hal-00566714, 24p., 2011.
6. J. Serra. *Image Analysis and Mathematical Morphology.* Academic Press, London, 1982.
7. P. Soille. *Morphological Image Analysis,* Springer-Verlag, Berlin, 1999.
8. C. Ronse. Ordering Partial Partition for Image Segmentation and Filtering: Merging, Creating and Inflating Blocks. Journal of Mathematical Imaging and Vision, 49(1):202–233, 2014.
9. P. Salembier J. Serra Flat Zones Filtering, Connected Operators, and Filters by reconstruction. IEEE Trans. on Images Processing, 4(8): 1153–60, 2014.